



**HAL**  
open science

# Thermal properties and radical monitoring after gamma, X-ray, and electron beam irradiation in polyamides

Blanche Krieguer, Nicolas Ludwig, Samuel Dorey, Nathalie Dupuy, Fabien Girard, Nina Girard-Perier, Florent Kuntz, Sylvain Marque

## ► To cite this version:

Blanche Krieguer, Nicolas Ludwig, Samuel Dorey, Nathalie Dupuy, Fabien Girard, et al.. Thermal properties and radical monitoring after gamma, X-ray, and electron beam irradiation in polyamides. *Physical Chemistry Chemical Physics*, 2024, 26 (31), pp.21222-21228. 10.1039/d4cp02358g . hal-04690441

**HAL Id: hal-04690441**

**<https://hal.science/hal-04690441v1>**

Submitted on 1 Oct 2024

**HAL** is a multi-disciplinary open access archive for the deposit and dissemination of scientific research documents, whether they are published or not. The documents may come from teaching and research institutions in France or abroad, or from public or private research centers.

L'archive ouverte pluridisciplinaire **HAL**, est destinée au dépôt et à la diffusion de documents scientifiques de niveau recherche, publiés ou non, émanant des établissements d'enseignement et de recherche français ou étrangers, des laboratoires publics ou privés.



Cite this: *Phys. Chem. Chem. Phys.*, 2024, 26, 21222

# Thermal properties and radical monitoring after gamma, X-ray, and electron beam irradiation in polyamides†

Blanche Krieguer,<sup>a</sup> Nicolas Ludwig,<sup>b</sup> Samuel Dorey,<sup>a</sup> Nathalie Dupuy,<sup>c</sup> Fabien Girard,<sup>c</sup> Nina Girard-Perier,<sup>a</sup> Florent Kuntz<sup>b</sup> and Sylvain R. A. Marque<sup>d</sup>

Ionizing radiation induced transformations in materials were monitored through tracking of the generation and degradation processes of radical species. Consequently, the types and quantities of radicals were determined by electron spin resonance (ESR). Subsequently, differential scanning calorimetry (DSC) was utilized to assess the impact of irradiation on the material crystallinity. The effects of gamma rays, X-rays, and electron beams were investigated on different polyamides, which exhibit an ESR signal up to 60 days. DSC results showed no significant effect of irradiation on the melting peak temperature of the materials, indicating that the amount of radicals generated was not large enough to induce a significant alteration of the material's macrostructure.

Received 10th June 2024,  
Accepted 22nd July 2024

DOI: 10.1039/d4cp02358g

rsc.li/pccp

## Introduction

Polymers play a crucial role in the pharmaceutical industry, being involved in a wide array of single-use medical devices such as syringes, gloves, and disposable plastic bags. Polymers can be of various natures depending on their applications and their desired properties.<sup>1</sup> Materials formulated from polyamides, known for their resistance to abrasion, chemicals, and corrosion, as well as their flexibility, are commonly used in cable ties,<sup>2</sup> tri-clamp unions and clamps among other components.

Gamma irradiation is used to sterilize almost half of the market of medical devices of biopharmaceutical single-use plastic systems.<sup>3,4</sup> With the pharmaceutical sector poised for rapid growth, there is a large strain to expand sterilization capacity.<sup>5</sup> The development of radiation sterilization alternatives to gamma rays is essential to manage the increasing volume of biopharmaceutical systems.<sup>1</sup> Currently, two alternative irradiation technologies are available: electron beam and X-ray irradiation.<sup>6–12</sup>

Electron-beam irradiation is a continuous process that utilizes an electron accelerator to convert electricity into a radiation beam. Electron accelerators can be used for direct electron beam irradiation or to produce X-ray fields which are generated through the Bremsstrahlung<sup>13</sup> effect generally in a tantalum converter. Both X-ray and gamma-rays are photons<sup>12</sup> but gamma-rays originate from radioactive sources and are emitted during disintegration. Due to their similar nature, X-ray and gamma-rays energy deposition patterns (dose profiles) are fairly similar resulting in a potentially easy conversion from gamma-rays to X-ray technologies.<sup>9–12</sup> X-ray may even achieve better dose uniformity because of their higher photon energy<sup>11</sup> and their easily tunable radiation field properties. In similarly irradiated material, electron beam exhibits much less penetration compared to photons as their interaction with matter is much stronger. Therefore, products packaging and/or geometry must be adapted for electron beam treatment when converting a gamma-ray irradiation process to an electron beam irradiation process.

From an interaction point of view, photon interaction with matter leads to the generation of secondary electrons through pair production, Compton effect and photoelectric effect<sup>14</sup> which will deposit their energy. Regardless of the irradiation technology, the electron will transfer its energy to the matter by ionizing or exciting processes. These interactions will lead to chemical bond breaking and will generate free radicals in polymers which are the seeds of material modification (cross-linking, chain scission, radiation oxidation, etc.).<sup>7,15,16</sup>

Electron spin resonance (ESR) is an effective technique for detecting radicals generated during irradiation and their

<sup>a</sup> Sartorius Stedim FMT S.A.S, Z.I. Les paluds, Avenue de Jouques CS91051, 13781, Aubagne Cedex, France. E-mail: blanche.krieguer@sartorius.com, samuel.dorey@sartorius.com

<sup>b</sup> Aerial, 250 Rue Laurent Fries, 67400 Illkirch, France

<sup>c</sup> Aix Marseille Univ, Avignon Univ, CNRS, IRD, IMBE, Marseille, France

<sup>d</sup> Aix Marseille Univ, CNRS, ICR, Case 551, 13397 Marseille, France. E-mail: sylvain.marque@univ-amu.fr

† Electronic supplementary information (ESI) available. See DOI: <https://doi.org/10.1039/d4cp02358g>



subsequent decay. As most radicals are unstable, they react rapidly.<sup>17,18</sup>

The impact of gamma irradiation on polyamide (PA) has already been investigated using ESR.<sup>17,19–21</sup> However, very few studies have compared the effects of gamma, e-beam and X-ray irradiations on polymers. The identification and quantification of post-irradiation radicals is essential to assess the similarity of effects on materials among the three irradiation technologies.

In our study, we investigated four different polyamide materials with varying formulations, including glass-reinforced PA, PA6.6, and PA12. We performed ESR analyses on each material for a period of 60 days after irradiation. The objective was to use ESR to monitor the free radicals generated by gamma, electron beam, and X-ray irradiations. Additionally, we performed differential scanning calorimetry (DSC) to compare the thermal properties of the irradiated PA, providing insights into changes in melting temperature regarding to the different types of irradiations. Hence, our approach provides data concerning the type, nature, and stability of radicals as well as the impact of irradiations on the thermal stability of the materials.

## Materials and methods

### Samples

The samples investigated (Fig. 1) are composed of various types of polyamides: glass-reinforced polyamide, polyamide 6.6 (PA6.6) and polyamide 12 (PA12). Table 1 gathers the typical density values provided by resin suppliers.<sup>22</sup>

### Samples packaging

The samples were packed in craft boxes at room temperature at Sartorius Stedim FMT S.A.S, Aubagne. This packaging along with the suitable arrangement of plastic components in thin craft boxes, ensured a uniform treatment. The dose uniformity was controlled by dosimetry.

### Samples irradiation

**Gamma rays.** Irradiation using gamma rays generated from <sup>60</sup>Co sources was carried out at Ionisos, Dagneux, France at an average dose rate of 1–2 kGy h<sup>-1</sup>. Irradiation was performed over several days by accumulation of the dose through many runs in the irradiation bunker.

**X-rays.** X-ray irradiation was performed at Aerial-CRT using the feerix<sup>®</sup> facility based on a Rhodotron (TT300 – IBA). A 7 MV X-ray beam is generated by converting a 7 MeV electron beam in a tantalum target. Irradiation was performed horizontally with

a pallet conveyor; several runs are realized in an X-ray field to realize a dose accumulation. Irradiation was conducted for one day with an average dose rate about 12 kGy h<sup>-1</sup>.

**e-beam.** E-beam irradiation was performed at Aerial-CRT using the same feerix<sup>®</sup> facility as for X-rays treatment. A 10 MeV vertical electron-beam was used with an average dose rate of 18 MGy h<sup>-1</sup> (5 kGy s<sup>-1</sup>). Irradiation was performed per lap of 50 kGy in order to avoid critical temperature elevation in the samples.

### Dosimetry

The targeted delivered doses were ≈ 50 kGy and ≈ 100 kGy with a target dose uniformity of ±10% and the Table 2 gathers the effective doses. To accurately measure the absorbed dose, alanine pellets combined with EPR spectroscopy (Magnettech MS5000 ESR, Bruker) were used with AerEDE<sup>®</sup> dosimetry software (Aerial, France). Dosimetry readings were taken in a manner that was traceable to an international standard.

The dosimeters were placed within the volume of the box containing samples to establish dose uniformity in the sample box.

### ESR measurements

ESR measurements were conducted using a Magnettech MS5000X ESR spectrometer manufactured by Bruker, Switzerland, and operated with ESR studio software for control. The samples were prepared from either irradiated dogbone specimens or part of irradiated products. Small pieces were cut to introduce them into a glass probe of 4.2 mm inner diameter. The samples, with a height of approximately 4 cm and a mass ranging from 100 to 200 mg, were then ready for analysis.

Firstly, the position of the signal was verified in a large magnetic field range (150–400 mT). Secondly the magnetic field range was narrowed from 320 mT to 340 mT around the sample, where the signal was present which is indicative of organic radicals. The spectra were recorded using a modulation amplitude of 0.2 mT, a sweep time of 60 seconds, and a single scan. Measurements were performed from 1 to 60 days after sample irradiation, at following days (D): D9, D15, D30, D60. During this time, samples were kept without light and at controlled temperature and humidity (25 °C and 45% RH).<sup>23</sup>

Signal amplitude (highest peak to peak signal) was measured on ESR spectra and calibrated using TEMPO (2,2,6,6-tétraméthylpipéridin-1-yl)oxy standard samples at spin concentration between 1 × 10<sup>16</sup> and 1 × 10<sup>19</sup> spin per g. TEMPO and standard samples were prepared according to the reported procedures.<sup>24</sup> TEMPO standards are very stable over time and the calibration curve was measured 8 times over several months in order to assess variabilities of measurements. Thus, ESR quantifications in this paper must be considered as TEMPO equivalent as the amplitude between TEMPO radical and probed radical in polymer may differ.

The ESR signals were measured for all PA samples prior to irradiation. The PA-4 sample was analyzed after gamma and X-ray irradiation at 50 kGy. The PA-1, PA-2, and PA-3 samples

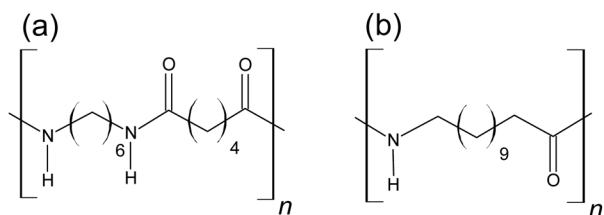


Fig. 1 Chemical structure of (a) polyamide 6.6 and (b) polyamide 12.



**Table 1** Non-irradiated PA commercially available (density)

Polymers	Polyamide (PA)			
Identification number	PA-1	PA-2	PA-3	PA-4
Type of polyamide	Glass reinforced PA	PA6.6	PA 12	PA6.6
Typical industrial application	Clamp/unions	Black cable tie	Black cable tie	Blue cable tie
Density (g cm <sup>-3</sup> )	1.38	1.14 <sup>a</sup>	1.01 <sup>a</sup>	1.14 <sup>a</sup>

<sup>a</sup> Standard density of polyamides 6, 6.6, and 12 are given in the literature.<sup>22</sup>

**Table 2** Effective doses on samples irradiated by gamma-rays, X-rays and e-beam

Target doses (kGy; ±10%)	Effective doses (kGy; ±10%)		
	Gamma	X-rays	e-beam
50	51	50	55
100	90	99	109

were analyzed after gamma, X-ray, and e-beam irradiation at 50 and 100 kGy.

### Differential scanning calorimetry (DSC)

Differential scanning calorimetry analyses were performed to characterize the physical and thermal properties of polymers. In a furnace, a thermocouple measures the temperature of the sample and another thermocouple measures one of the references (empty crucible). The heat variations observed during the glass transition and the melting temperature were also measured and a thermogram was established using these data. DSC tests were performed using a Sensys Evo131 thermal analyzer from Setaram.

For the DSC analysis, 3 cycles (heating and cooling) were performed on ~20 mg. The range of heating was -50 to 200 °C. The ramp of temperature was 10 °C min<sup>-1</sup> and a stabilization step was set before and after each cycle. For the results interpretation, only the 2nd and the 3rd cycles were considered, since the first cycle was performed to erase the thermal past of the material. The melting peak temperature and the melting onset temperature were both integrated and determined using the Calisto Processing software.

### Equivalency analysis

**ESR.** Regression models were performed using the Minitab software to assess the effect of doses (50 and 100 kGy), the effect of ageing after irradiation, and the effect of the three irradiation technologies on the spin per mg values measured by ESR for each sample. This model allows for the evaluation of the significant impact of each independent variable, with confidence interval at 95% ( $\alpha = 0.05$ ).

**DSC.** To assess the equivalency between gamma, X-rays, and e-beam irradiated samples, equivalence tests (TOST, two one-sided *t*-test<sup>25</sup>) were performed with Minitab<sup>®</sup> software. The melting peak and melting onset temperatures of the samples either irradiated by Gamma, X-ray or e-beam were considered equivalent if results were within the equivalence interval

defined with equivalency criterium ( $\pm 5$  °C) confidence interval at 95% ( $\alpha = 0.05$ ).

## Results and discussion

### Electron spin resonance

ESR was performed after gamma, X-ray and e-beam radiation at 50 and 100 kGy for PA-1, PA-2 and PA-3. PA-4 was analyzed by gamma and X-ray at 50 kGy.

The literature describes a well-defined multiplet ESR signal for polyamide when ESR analysis is performed immediately following gamma irradiation.<sup>17,26,27</sup> In our case, Fig. 2 displays the ESR signal of polyamide samples one day after exposure to X-rays and e-beam at 100 kGy. Prior to irradiation, a broad singlet was observed in PA-2 and PA-3, in sharp contrast to PA-1.

Both PA-1 and PA-2 exhibit similar ESR signals as depicted in Fig. 2, while PA-3 displays a poorly resolved signal that more closely aligns with those reported in the literature. The ESR pattern observed for PA-1-3 is presumed to result from the superimposition of two signals: a multiplet ascribed to the radical  $-\text{CH}_2\text{CONHC}^*\text{HCH}_2-$  and a singlet present in the polymer prior to irradiation.

In our study, the alkyl radical is only detected after X-ray and e-beam irradiation because ESR measurements are performed within one day post-irradiation. In contrast, measurements after gamma irradiation are performed several days later due to the time required for sample transportation.

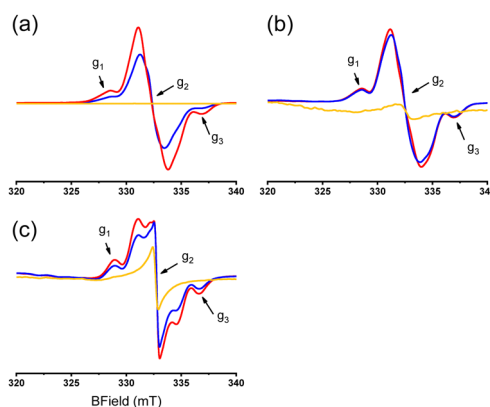


**Fig. 2** Signal of (a) PA-1, (b) PA-2 and (c) PA-3, non-irradiated (yellow line) and one day after irradiation at 100 kGy by X-rays (red line) and e-beam (blue line). Arrows are to point peaks corresponding to the expected radical ( $g \approx 2.003$ ).



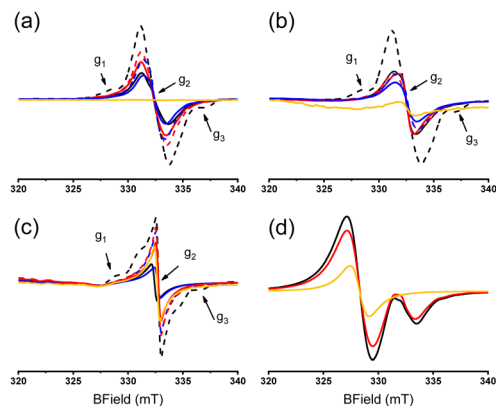


Fig. 3 Signal of (a) PA-1, (b) PA-2, (c) PA-3 and (d) PA-4, non-irradiated (yellow line) and nine days after irradiation at 50 kGy (solid line) and 100 kGy (dotted line) by gamma irradiation (black line), X-rays (red line) and e-beam (blue line). Arrows are to point peaks corresponding to the expected radical ( $g \approx 2.003$ ).

Fig. 3 displays the ESR signal of polyamide samples nine days after exposure to gamma, X-rays, and e-beam at 50 and 100 kGy. For PA-1, PA-2 and PA-3, a singlet is observed for gamma, e-beam and X-rays regardless of the dose. The singlet signal is attributed to the radical  $-\text{CH}_2\text{CHO}^\bullet\text{NHCH}_2-$  ( $g = 2.003$ ).<sup>17,28</sup>

After gamma irradiation at 100 kGy, a small signal was detected and ascribed to the expected multiplet radical, *i.e.*  $-\text{CH}_2\text{C}^\bullet\text{HCONHCH}_2-$ .<sup>17,26,29</sup> Similar signals are observed for other samples aged after irradiation and are reported in Fig. S1 (ESI†).

PA-4 displays two radical species (Fig. 3d), with the signal at  $g = 2.03$  being observed before irradiation and does not decaying upon ageing (Fig. 3d and Fig. S1, ESI†). According to the literature,<sup>30,31</sup> the signal at  $g = 2.03$  can be tentatively ascribed to the blue additive, which likely contains a sulfur-centered radical. For industrial reasons the formulation of the material cannot be obtained. The second weak signal of PA-4 (Fig. 3d) perfectly matches the singlet observed in PA-1, PA-2 and PA-3.

Fig. 4 displays the concentration of radicals for each PA and the maximum concentration is reported in Table 3. The ESR signal and the quantity of radicals generated exhibit a decrease after irradiation, a trend that holds across the different irradiation technologies applied to samples PA-1 and PA-2. The amount of radicals remains constant in PA-3 nine days after irradiation (Fig. 4).

For PA-4, the sulfur radical maintains a constant concentration within the formulated polymer, and due to its predominance, the kinetics of the singlet radical cannot be observed with the technique utilized.

Radical levels in samples exposed to gamma, X-ray, and e-beam irradiation at doses of 50 kGy and 100 kGy were monitored for a period of up to 60 days post-irradiation.

Regression models were developed for each sample to determine the influence of dose, ageing, and irradiation technology on radical production. These models allow us to assess whether the dose, ageing after irradiation, and irradiation technologies can have a significant effect on the quantity of

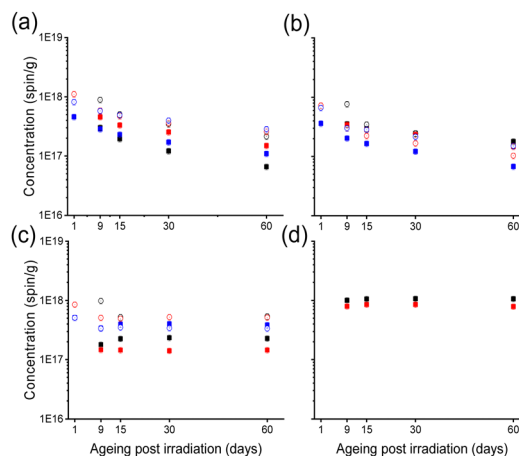


Fig. 4 Monitoring of the concentration of radicals for each PA sample by ESR as concentration (spin per g) vs. ageing (days). (a) PA-1. (b) PA-2. (c) PA-3. (d) PA-4. Filled squares correspond to samples irradiated at 50 kGy and open circles correspond to samples irradiated at 100 kGy, black for gamma irradiation, red for X-rays and blue for e-beam.

Table 3 Maximum radical concentration ( $C_{\text{max}}$ , spin per g) in polyamide samples

Irradiation technology	Dose (kGy)	Maximum radical concentration (spin per g; in $10^{17}$ )			
		PA-1	PA-2	PA-3	PA-4
Gamma	50	3	4	2	10
	100	8	8	10	n.a. <sup>a</sup>
X-ray	50	5	3	1	8
	100	6	3	5	n.a. <sup>a</sup>
e-beam	50	3	2	5	n.a. <sup>a</sup>
	100	6	3	5	n.a. <sup>a</sup>

<sup>a</sup> n.a.: non available data.

radicals generated in the sample. Indeed, with  $p$ -values less than 0.05, it indicates a significant effect. The Pareto chart shows the absolute values of the standardized effects from the largest to the smallest effect. The chart also plots a reference line that indicates if the effects are statistically significant. The reference line for statistical significance depends on the significance level (denoted by  $\alpha$ ). The significance level is 1 minus the confidence level for the analysis.<sup>32</sup>

Post-irradiation time (*i.e.*, kinetics) shows a significant effect, with radical levels decreasing with increasing post-irradiation time for PA-1 and PA-3 (Fig. 5a and c). For the PA-1 and PA-2 samples (Fig. 5a and c), an increase in dose was correlated with a rise in radical concentration.

When comparing X-ray and e-beam with gamma irradiation, the Pareto charts for each sample showed no notable differences among the irradiation technologies. The equations and coefficients of the regression models obtained for each sample are reported in ESI†. No regression model was generated for PA-4 due to the lack of data.

### Thermal properties (DSC)

The PA-2 and PA-4 samples are formulated from polyamide 6.6, while the PA-3 sample is formulated from polyamide 12.





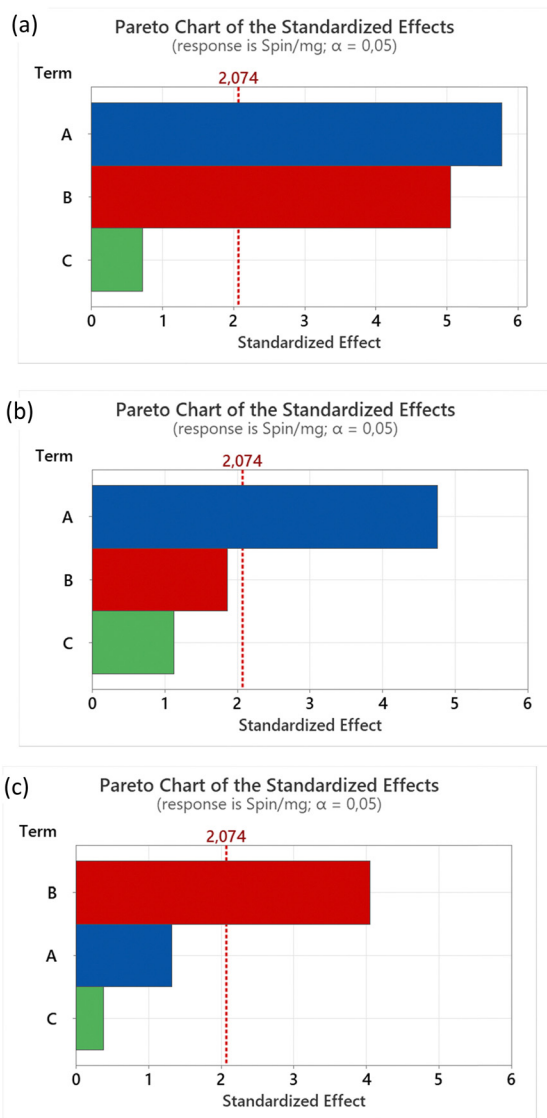


Fig. 5 Pareto analysis of significant effects on radical concentration: ageing after irradiation (term A in blue), dose (term B in red) and irradiation technologies (term C in green). (a) PA-1. (b) PA-2. (c) PA-3.

PA6.6 has a higher crystallinity than PA12. This is attributed to the higher hydrogen-bonding density in PA6.6, which facilitates faster crystallization compared to PA12. Despite PA12 having a more flexible chain structure, which could potentially lead to faster crystallization at lower temperatures, PA6.6 still crystallizes slightly faster than PA12.<sup>33</sup>

The DSC results (Fig. 6) regarding the evaluation of the thermal properties of polyamide show that the melting temperature of the PA-1, PA-2 and PA-4 samples (PA6.6) is about 260 °C, while for PA-3 (PA12), the melting temperature is about 180 °C; these results are consistent with the literature.<sup>34–37</sup>

The melting temperatures of PA remain consistent regardless of the irradiation technology used (at 50 and 100 kGy) and correspond to the values reported for non-irradiated materials. This indicates that their thermal properties are unchanged. Consequently, the structure of the materials is not altered, and

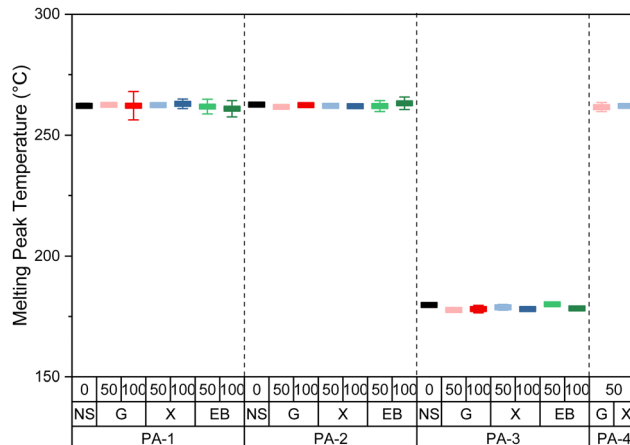


Fig. 6 Melting peak temperature for all PA samples non irradiated (black) and irradiated by gamma (red), X-ray (blue) and e-beam (green) at 50 and 100 kGy.

their thermal properties are not affected. Examples of thermograms and melting onset temperature are displayed in ESI.†

## Conclusions

Electron spin resonance measurements were used to investigate the radicals generated in these polymers when exposed to different sources of radiation. The results indicate that the type of radicals generated is similar for all PA but the presence of additives can also affect the ESR signals. Indeed, alkyl radicals were present in all PA samples. No significant differences in radical concentration were found when comparing the effects of gamma, e-beam, and X-ray irradiation on these materials.

The generation and decay of free radicals in PA appeared equivalent, even though the specific radicals varied.

The thermal properties of polyamides were also investigated using DSC, and no significant differences were observed in the melting temperature regardless of the irradiation technologies or the doses.

The objective was to determine whether the type of radiation source influences the radicals generated during material interaction. The lack of differences suggests that the behavior of the materials after irradiation is likely to be similar regardless of the radiation source used. The melting temperature, the ESR signals uniformity, the kinetics decay and the radical concentration profiles with gamma, e-beam, and X-rays in PA lend credence to the hypothesis of a standardized radiation interaction with condensed matter.

## Data availability

The data supporting this article have been included as part of the ESI.†

## Conflicts of interest

There are no conflicts to declare.



## Acknowledgements

N. D., F. G. and S. R. A. M. are thankful to Aix-Marseille Université (AMU), Institut de Recherche pour le Développement (IRD) and Centre National pour la Recherche Scientifique (CNRS) for support.

## Notes and references

- BPAS Technical Guide, X-rays Sterilization of single-Use BioProcess Equipment, Part 1: Industry Need, Requirements & Risk Evaluation, 2021.
- S. A. Umoren, M. M. Solomon and V. S. Saji, *Polymeric Materials in Corrosion inhibition fundamentals and applications*, 2022, pp. 541–563.
- N. Girard-Perier, M. Claeys-Bruno, S. R. A. Marque, N. Dupuy, F. Gaston and S. Dorey, Effects of X-ray, electron beam and gamma irradiation on PE/EVOH/PE multilayer film properties, *Chem. Commun.*, 2021, 57, 11049–11051.
- N. Dupuy, S. R. A. Marque, L. S. Fifield, M. Pharr, D. Staack, S. D. Pillai, L. Nichols, M. K. Murphy and S. Dorey, Supplementing Gamma Sterilization with X-Ray and E-Beam Technologies, *Bioprocess Technol.*, 2022, 20, 24–28.
- M. Wellesley, BBC publishing, 2020.
- P. M. Armenante and O. Akiti, in *Chemical Engineering in the Pharmaceutical Industry*, ed. D. J. Am Ende and M. T. Am Ende, John Wiley & Sons, Inc., Hoboken, NJ, USA, 2019, pp. 311–379.
- D. Darwis Erizal, B. Abbas, F. Nurlidar and D. P. Putra, Radiation Processing of Polymers for Medical and Pharmaceutical Applications, *Macromol. Symp.*, 2015, 353, 15–23.
- S. Moondra, N. Raval, K. Kuche, R. Maheshwari, M. Tekade and R. K. Tekade, *Dosage form design parameters*, Elsevier, 2018, pp. 467–519.
- H. de Brouwer, Comparison of the effects of x-ray and gamma irradiation on engineering thermoplastics, *Radiat. Phys. Chem.*, 2022, 193, 109999.
- B. Croonenborghs, M. A. Smith and P. Strain, X-ray versus gamma irradiation effects on polymers, *Radiat. Phys. Chem.*, 2007, 76, 1676–1678.
- T. K. Kroc, Monte Carlo simulations demonstrating physics of equivalency of gamma, electron-beam, and X-ray for radiation sterilization, *Radiat. Phys. Chem.*, 2023, 204, 110702.
- K. Makuuchi and S. Cheng, *Radiation Processing of Polymer Materials and its Industrial Applications*, John Wiley & Sons, Inc., Hoboken, NJ, USA, 1st edn, 2012.
- G. Sadler, W. Chappas and D. E. Pierce, Evaluation of e-beam,  $\gamma$ - and X-ray treatment on the chemistry and safety of polymers used with pre-packaged irradiated foods: a review, *Food Addit. Contam.*, 2001, 18, 475–501.
- Applications of ionizing radiation in materials processing*, ed. A. G. Chmielewski and Y. Sun, Institute of Nuclear Chemistry and Technology, Warszawa, 2017, vol. 1.
- J. Ahmed, J. Wu, S. Mushtaq and Y. Zhang, Effects of electron beam irradiation and multi-functional monomer/co-agents on the mechanical and thermal properties of ethylene-vinyl acetate copolymer/polyamide blends, *Mater. Today Commun.*, 2020, 23, 100840.
- M. Morino, Y. Nishitani, T. Kitagawa and S. Kikutani, Thermal, Mechanical and Tribological Properties of Gamma-Irradiated Plant-Derived Polyamide 1010, *Polymers*, 2023, 15, 3111.
- P. Simon, A. Rocketm and M. Azori, ESR Study Of  $\gamma$ -Irradiated Nylon-6; Conformational Isomerism Of Free Radicals, *Eur. Polym. J.*, 1977, 13, 189–192.
- M. I. Chipara, ESR investigations on ion beam irradiated polymers, *Nucl. Instrum. Methods Phys. Res., Sect. B*, 1997, 131, 85–90.
- R. Tian, K. Li, Y. Lin, C. Lu and X. Duan, Characterization Techniques of Polymer Aging: From Beginning to End, *Chem. Rev.*, 2023, 123, 3007–3088.
- H. Yoshida and B. Rånby, Electron spin resonance studies on oriented polyoxymethylene, *J. Polym. Sci., Part A: Gen. Pap.*, 1965, 3, 2289–2302.
- A. Oshima, T. Seguchi and Y. Tabata, Radiation-induced free radicals and their behaviour in crosslinked polytetrafluoroethylene (PTFE), *Polym. Int.*, 1999, 48, 996–1003.
- P. A. Polyamides, <https://www.techniques.ingenieur.fr/base-documentaire/materiaux-th11/matieres-thermoplastiques-monographies-42147210/polyamides-pa-a3360/>, accessed May 31, 2024.
- B. Krieguer, S. R. A. Marque, S. Dorey, N. Dupuy, F. Girard, N. Girard-Perier, F. Kuntz and N. Ludwig, Radical detection and electron-spin resonance (ESR) monitoring in polymer materials irradiated with gamma and X-rays: Polyethylene and polypropylene, *J. Appl. Polym. Sci.*, 2024, e55098.
- G. Audran, S. Dorey, N. Dupuy, F. Gaston and S. R. A. Marque, Degradation of  $\gamma$ -irradiated polyethylene-ethylene vinyl alcohol-polyethylene multilayer films: An ESR study, *Polym. Degrad. Stab.*, 2015, 122, 169–179.
- Y. Ni, T. T. Bisel, M. K. Hasan, D. Li, W. K. Fuchs, S. K. Cooley, L. Nichols, M. Pharr, N. Dupuy, S. R. A. Marque, M. K. Murphy, S. D. Pillai, S. Dorey and L. S. Fifield, Compatibility of ethylene vinyl acetate (EVA)/ethylene vinyl alcohol (EVOH)/EVA films with gamma, electron-beam, and X-ray irradiation, *npj Mater. Degrad.*, 2023, 7, 93.
- C. T. Graves and M. G. Ormerod, The Radiation Chemistry of Some Polyamides, *Electron Spin Reson.*, 1963, 4, 81–91.
- B. Li and L. Zhang, Dependence of decaying of trapped radicals on aggregates of polyamide 1010, *Radiat. Phys. Chem.*, 1997, 49, 395–397.
- A. G. Davies, J. A. Howard and M. Lehnig, *Magnetic properties of free radicals- Organic O-, P-, Se-, Si-, Ge-, Sn-, Pb-, As-, Sb-Centered Radicals*, 1979, vol. 9c2.
- H. Paul, H. Fischer and A. Berndt, *Magnetic properties of free radicals- Organic C-Centered Radicals*, 1977, vol. 9b.
- N. Gobeltz, A. Demortier, J. P. Lelieur and C. Duhayon, Correlation between EPR, Raman and colorimetric characteristics of the blue ultramarine pigments, *Faraday Trans.*, 1998, 94, 677–681.
- S. D. McLaughlan and D. J. Marshall, Paramagnetic resonance of sulfur radicals in synthetic sodalites, *J. Phys. Chem.*, 1970, 74, 1359–1363.



- 32 Minitab software.
- 33 T. Wang, X. Li, R. Luo, Y. He, S. Maeda, Q. Shen and W. Hu, Effects of amide comonomers on polyamide 6 crystallization kinetics, *Thermochim. Acta*, 2020, **690**, 178667.
- 34 J. Simek, V. Dockalova, Z. Hrdlicka and V. Duchacek, Effect of liquid butadiene rubber on mechanical properties of polyamide 11/polyamide 12 blends, *J. Polym. Eng.*, 2015, **35**, 349–357.
- 35 H. Ghasemi, A. Mirzadeh, P. J. Bates and M. R. Kamal, Effect of Polyamide 66 on the Mechanical and Thermal Properties of Post-Industrial Waste Polyamide 6, *Polym.-Plast. Technol. Eng.*, 2014, **53**, 1794–1803.
- 36 C. Menchaca, A. Alvarez-Castillo, G. Martinez-Barrera, H. Lopez-Valdivia, H. Carrasco and V. M. Castano, Mechanisms for the modification of nylon 6,12 by gamma irradiation, *IJMPT*, 2003, **19**, 521.
- 37 M. C. Evora, L. D. B. Machado, V. L. Lourenço, O. L. Gonçalez and H. Wiebeck, Thermal Analysis of Ionizing Radiation Effects on Recycled Polyamide-6, *J. Therm. Anal. Calorim.*, 2002, **67**, 327–333.

